Tool Chatter Diagnosis using EMD and LMD Techniques: A Comparative Study

Gupta, Pankaj
Jaypee University of Engineering and Technology, Guna (M.P.)

Singh, Bhagat
Jaypee University of Engineering and Technology, Guna (M.P.)

Shrivastava, Yogesh
Galgotias College of Engineering and Technology, Greater Noida

https://doi.org/10.5109/7183427

出版情報：Evergreen. 11 (2), pp.1216-1226, 2024-06. 九州大学グリーンテクノロジー研究教育センター
バージョン：

Tool Chatter Diagnosis using EMD and LMD Techniques: A Comparative Study

Pankaj Gupta[1*], Bhagat Singh[1], Yogesh Shrivastava[2]
[1]Jaypee University of Engineering and Technology, Guna (M.P.), India
[2]Galgotias College of Engineering and Technology, Greater Noida, India

*Author to whom correspondence should be addressed:
E-mail: pankajguptamech88@gmail.com

(Received September 14, 2022; Revised April 8, 2024; Accepted June 14, 2024)

Abstract: Downtime, poor surface quality, excessive noise, dimension inaccuracy, and disproportionate tool wear are all negative effects of the regenerative chatter phenomena. On obtained audio signals generated during machining of Al-6061-T6, empirical mode decomposition (EMD) and local mean decomposition (LMD) techniques are performed, followed by rapid Fourier transform (FFT). In order to detect and evaluate chatter in its early stages, these decomposed signals are examined to extract tool chatter traits by analysing different statistical indicators such as kurtosis, absolute mean amplitude, impulse index, root mean square value, and so on. The Nakagami probability distribution is used to determine statistical indicator threshold limits. According to the results of the investigation, LMD is a more efficient technique than EMD.

Keywords: Nakagami distribution; tool chatter; EMD; LMD; statistical parameters; non-stationary signal processing.

1. INTRODUCTION

Inhomogeneity of the workpiece causes regenerative chatter, resulting in an uneven cut surface [1)]. With each passing turning pass, the uneven waviness of the surface becomes more pronounced [2,3)]. When a tool goes from one profile to another during successive turning passes, it experiences a sudden jerk, causing tool vibration, which is commonly referred to as tool chatter [4)]. Figure 1 depicts a symmetric rendition of the wavy profile. The original surface of the workpiece before cutting is shown in Fig 1. During chatter initiation, the intermediate surface represents the workpiece's surface. The wavy surface formed by self-excited vibration is represented by the final surface.

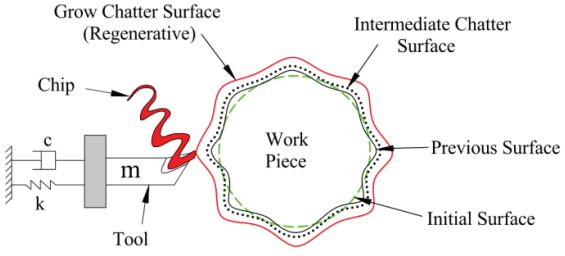

Fig. 1 Schematic representation of wavy profile

Poor surface quality, high tool wear, and a reduced production rate are all consequences of regenerative chatter [5,6)]. As a result, it is critical for researchers to diagnose and reduce chatter in order to mitigate its negative impacts [7,8)]. Many studies have used in-process monitoring approaches, but others have favoured in-cycle monitoring techniques [9,10)].

In-process monitoring has various advantages over the other two systems since it may provide information and details at any point during the machining process [11,12,13)]. The contact type of monitoring and the non-contact type of monitoring are the two basic types of in-process monitoring [14,15)]. Researchers also discovered that captured raw chatter signals contain ambient noise, making it difficult to determine the exact nature of talk. To filter out these contaminations before the diagnosing tool chatters, a suitable signal processing mechanism must be implemented [16)]. The sensor and signal types gathered determine which filtering signal processing approach to use. Researchers have developed numerous signal processing algorithms for processing chatter signals in the previous decade, such as wavelet transform, empirical mode decomposition, and Hilbert transform [18,19)]. They discovered that while the EMD technique is quite effective in locating the chatter band, it is prone to modal aliasing, which occurs when an IMF comprises distinct time scales, or comparable time scales scattered across different IMFs [20)]. As a result, identifying the specific buzz band is challenging. Furthermore, applying the Hilbert transform to the EMD decomposition results in in negative instantaneous frequency and serious end effect occurrence.

Smith's local mean decomposition technique was used to solve this problem to a considerable extent [21]. LMD lowers the decomposition's end consequences and prevents the over-enveloping issue. LMD is a time–frequency analysis approach that is more moderate than EMD [22,23]. Its product functions include more frequencies, and the envelope data provides a significant quantity of chatter data. EMD and LMD techniques were used to process the audio chatter signals that were collected [24,25,26].

The statistical indicators were then analysed for both notable IMFs and PFs in the next stage. These statistical indicators were also examined for recognising chatter features and the suitability of the EMD and LMD techniques for processing chatter signals. Furthermore, the acquired results were confirmed using a theoretical stability lobe diagram and were also used to determine the commencement of chatter. Based on the findings, it can be concluded that the LMD is superior to the EMD.

2. PROPOSED METHODOLOGY

The process has been divided into four parts for easier understanding, as illustrated in Fig. 2. Machine, tool-workpiece, and machining settings were all chosen in the initial stage. The microphone was used in the second stage to collect conversation signals. The recorded chatter signals were preprocessed using EMD and LMD, followed by the Fourier transform of IMFs and PFs, respectively, in the third stage to identify the mode largely responsible for chatter. Following that, statistical indicators for both important IMFs and PFs were analysed in the next stage. These statistical variables were also examined for chatter features and the suitability of EMD and LMD for processing chatter signals. A theoretical stability lobe diagram is also used to verify the results.

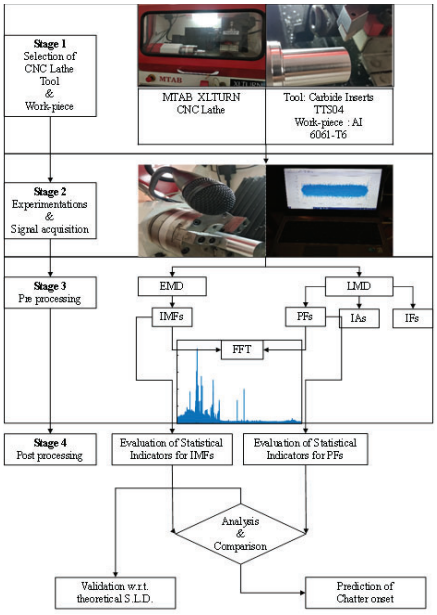

Fig. 1: Outlay of the proposed methodology

2.1 EXPERIMENTATION DETAILS

Turning trials were carried out on the MTAB XL-TURN CNC lathe in this study. Al-6061-T6 was chosen as the work material. A carbide insert TTS04 is used for the turning process. Figure 3 depicts the machining conditions used, as well as the input settings and microphone specifications.

Specification of Microphone

Model	AHUJA AGN-480
Specialty	Dynamic Unidirectional Microphone
Frequency Response	50-10,000 Hz
Sensitivity	2.0 mV/Pa
Impedance	600 ?
Overall Length	470 mm

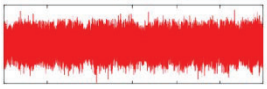

Input parameters and their levels

S. No.	Parameters	Level 1	Level 2	Level 3
1.	Depth of cut, d (mm)	0.2	0.3	0.4
2.	Spindle speed, n (rpm)	1000	1500	2000
3.	Feed, f (mm/min)	30	35	40

Fig. 2: Machining condition, input settings and microphone specifications

2.2 THEORETICAL ANALYSIS

2.2.1 Processing of acquired signals using Empirical mode decomposition (EMD)

Ambient noise is contained in raw chatter signals, making it difficult to determine the true nature of chatter. Before the diagnosis tool chatter, the empirical mode decomposition (EMD) signal processing approach filters out these contaminations. Huang invented the EMD technique[10]. It took the chatter signals and decomposed them into intrinsic mode functions (IMFs). The algorithm of EMD has been described in Fig. 4[11]. Simple oscillatory functions with variable amplitude and frequency are known as IMFs. These IMFs must meet the following requirements.:

a. The number of IMF extrema and zero-crossings must be the same or differ by no more than one.
b. The envelopes formed from the local extrema should have a mean value of zero.

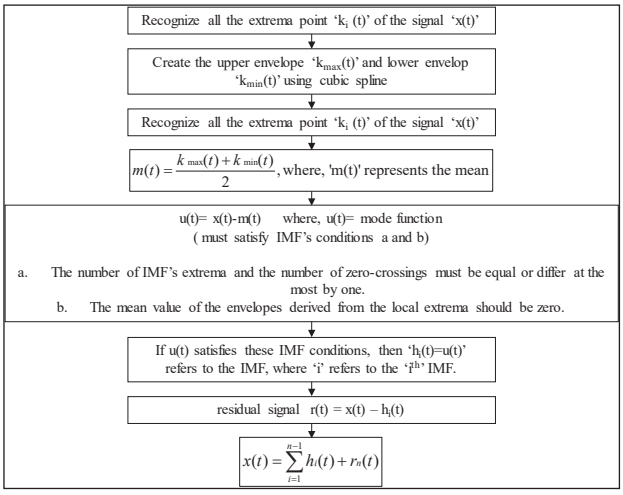

Fig. 3: Empirical mode decomposition steps

All conversation signals were demodulated into a number of IMFs using the EMD methods described above. Figure 5 shows the Fast Fourier transform (FFT) of a critical IMF of one of the signals carrying chatter information. For all 27 tests, these IMFs are investigated and the degree of chatter is assessed using statistical metrics

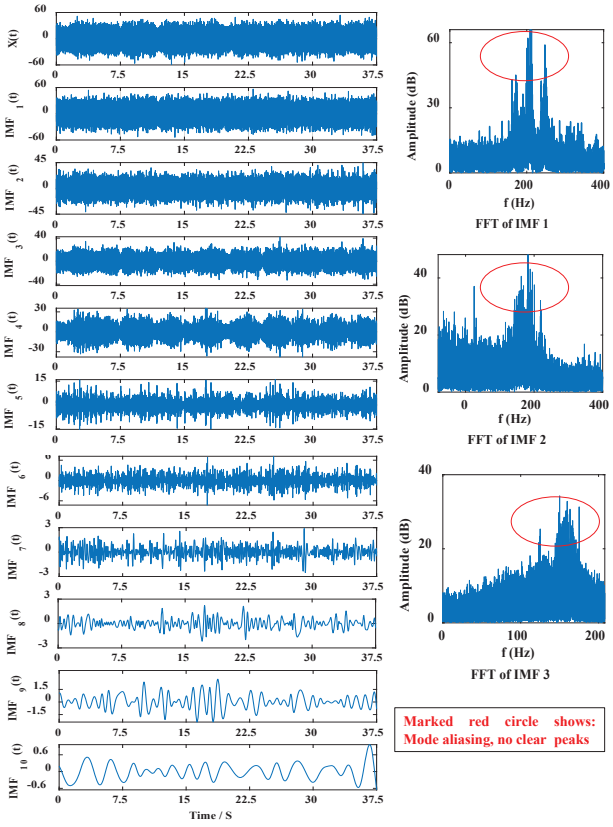

Fig. 1 IMFs & FFTs at depth of cut =0.3 mm, spindle speed =2000 rpm, feed rate =40 mm/min.

Several challenges arise when using the EMD approach to process signals. Due to a modal aliasing issue, it misinterpreted the chatter frequencies. This approach also fails to distinguish between closed and weak frequency signal components, as seen in Fig. 5. Because EMD has mode aliasing concerns in high frequency signals, which are typical of chatter signals, it is best suited for low frequency transmissions. As a result, the authors evaluated a new adaptive strategy, the LMD technique. The chatter signals were decomposed by LMD into a number of product functions, which are explained in the next section.

2.2.2. Processing of acquired signals using local mean decomposition (LMD)

The signal processing technique of local mean decomposition (LMD) has been modified to filter out contaminations before the diagnosis tool chatter. Figure 6 depicts the processes involved in the LMD approach. The critical PFs holding the chatter information were then designated using Fast Fourier Transform (FFT) as illustrated in Fig. 7.

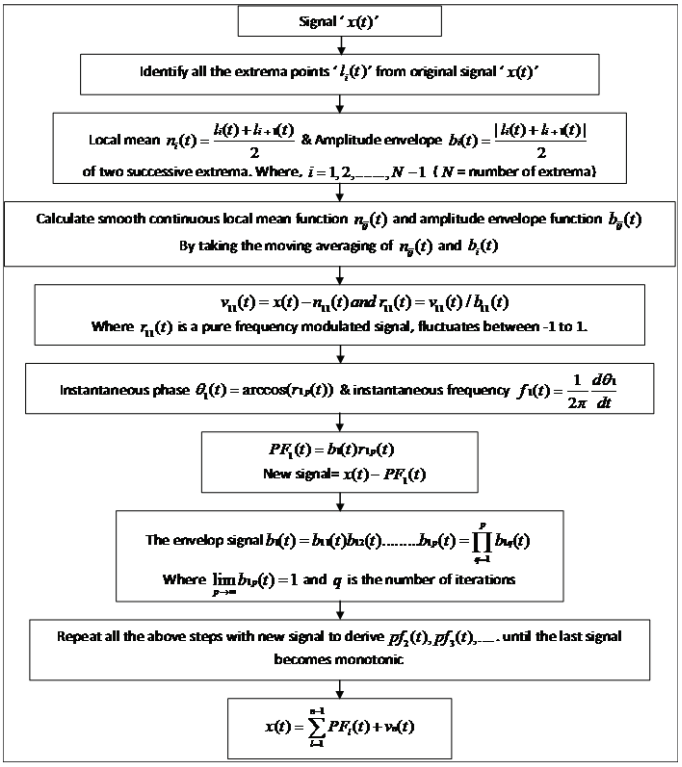

Fig. 6: Local mean decomposition steps

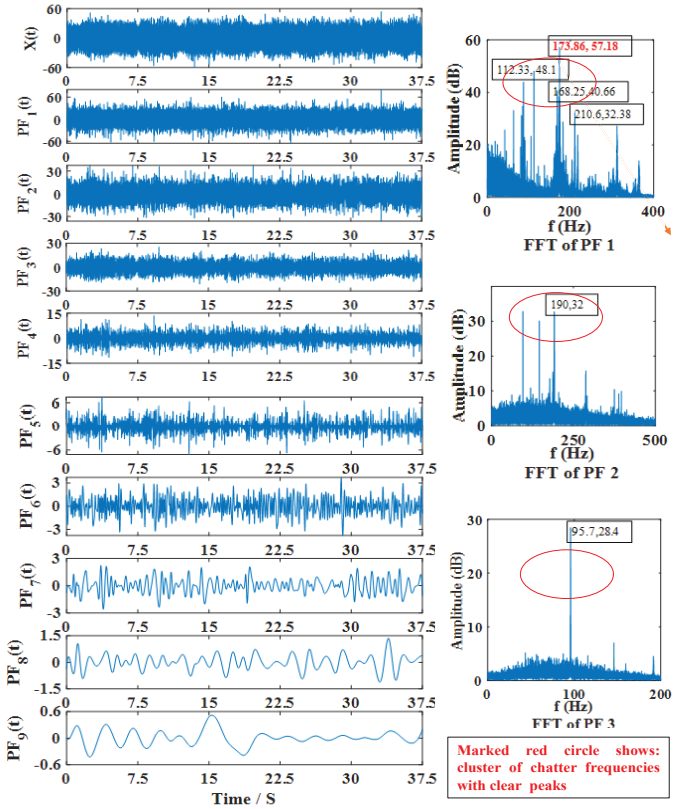

Fig. 2 PFs & FFTs at depth of cut=0.3 mm, spindle speed=2000 rpm, feed rate=40 mm/min.

Statistical chatter parameter's analysis

Large variations are visible in a short time during the transition from stable to chatter, and fluctuations rise progressively, which could be represented by time domain statistical chatter characteristics. The commencement of chatter is invariably accompanied by a shift in the frequency spectrum. Many statistical chatter metrics have been used in the chatter severity analysis. All indicator values for all 27 studies were determined using the statistical indicators indicated in Table 1. Table 2 displays the parameters derived for EMD-preprocessed signals, while Table 3 shows the parameters calculated for LMD-preprocessed signals.

Table 1. Indicators

Feature name	Expression	Definition	Effect
Standard deviation	$\sigma = \sqrt{\frac{1}{N}\sum_{n=1}(x(t)-\mu)^2}$ where x(t) = signal, N = length of signal, μ= mean	Standard deviation represents the deviation of the signal from the mean .	Higher the value, more will be the chatter
Root mean square value	$x_{rms}(t) = \sqrt{\frac{1}{N}\sum_{n=1}^{N} x(t)^2}$ where x(t) = signal, N = length of signal	The signal's energy content is represented by the root mean square (RMS). When two independent sources of noise are combined, the RMS value equals the total of their respective RMS values.	Higher the value, larger the chatter component
Peak to peak value	$x(t)_p$= max(x(t)) - min(x(t) where x(t) = signal	From crest to trough, the signal's peak to peak value is measured.	The chatter will get more intense as the peak to peak value increases.
Kurtosis index	*where* $\sigma = \sqrt{\frac{1}{N}\sum_{n=1}^{N}\left((x(t)-\overline{x(t)}\right)^2}$ where x(t) = signal, N = length of signal σ = standard deviation	Kurtosis is the measurement of a signal's peak-ness. Leptokurtic signals have a reasonably high peak, platykurtic signals have a flat top, and mesokurtic signals have a signal that is neither very peaked nor particularly flat-topped.	If the value is leptokurtic, it indicates a lot of talk. If the number is mesokurtic, it suggests there is chatter but it isn't as intense. If the kurtosis value is platykurtic, the machining is stable.
Waveform index	$N\sum_{n=1}$ $x_a(t)$ = absolute mean amplitude of the signal x(t) = signal, N = length of signal	The waveform index is the ratio of the signal's RMS value to its absolute mean amplitude.	The larger the chatter component, the higher the value.
Peak index	$I_i = \overline{x_{rms}(t)}$ Where,x_{rms}(t) = RMS value , x(t) = signal	The peak index is calculated as the ratio of the signal's greatest absolute value to its RMS value.	The larger the chatter component, the higher the value.
Impulse index	$I_i = \frac{\max(x(t))}{x_a(t)}$ Where,x_a(t)= absolute mean amplitude x(t) = signal	The ratio of the signal's maximum absolute value to its absolute mean amplitude is the impulse index.	The larger the chatter component, the higher the value.
Margin index	$\left(N\sum_{n=1}\right.$ Where, x_s(t) = root square amplitude of the signal x(t) = signal, N = length of signal	The margin index is the ratio of the signal's greatest absolute value to its root square amplitude.	The larger the chatter component, the higher the value.
Absolute mean amplitude	$AMA = \frac{1}{N}\sum_{n=1}^{N}\lvert x(t)\rvert$	The absolute value of chatter amplitudes is averaged.	The higher the AMA value, the more chatter components in the signal.

Table 2. Statistical indicators of prominent IMFs

Exp. No.	(d) mm	(n) rpm	(f) mm/min	Standard deviation	RMS value	Peak-to-peak value	Kurtosis index	Waveform index	Peak index	Impulse index	Margin index	Absolute mean amplitude
1	0.2	1000	30	1.3	1.3	12.6	3.283	1.276	5.313	6.778	8.108	0.992
2	0.2	1000	35	0.6	0.6	6.9	3.571	1.284	5.363	6.887	8.264	0.489
3	0.2	1000	40	1.3	1.3	12.9	3.691	1.316	4.674	6.153	7.525	0.985
4	0.2	1500	30	2	2	17.7	3.297	1.292	4.397	5.481	6.882	1.535
5	0.2	1500	35	1.4	1.4	12.4	2.919	1.254	4.031	5.055	5.994	1.113
6	0.2	1500	40	2	2	20.5	3.347	1.290	4.931	6.361	7.695	1.583
7	0.2	2000	30	3.3	3.3	31.5	3.541	1.306	5.637	7.360	8.948	2.509
8	0.2	2000	35	3.9	3.9	32.4	3.645	1.316	4.153	5.465	6.684	2.981
9	0.2	2000	40	4.4	4.4	39.3	3.657	1.320	4.731	6.243	7.657	3.339
10	0.3	1000	30	1.4	1.4	14.8	3.495	1.287	5.444	7.006	8.422	1.054
11	0.3	1000	35	0.6	0.6	5.6	3.325	1.276	4.525	5.773	6.911	0.487
12	0.3	1000	40	0.1	0.1	0.8	4.343	1.369	3.040	4.161	5.187	0.089
13	0.3	1500	30	0.1	0.1	0.8	2.842	1.269	2.783	3.532	4.233	0.113
14	0.3	1500	35	1.5	1.5	12.2	2.928	1.251	3.900	4.880	5.780	1.213
15	0.3	1500	40	1.4	1.4	10.9	2.995	1.257	3.826	4.808	5.703	1.121
16	0.3	2000	30	4.5	4.5	36.2	3.369	1.303	4.030	5.253	6.398	3.454
17	0.3	2000	35	4.5	4.5	39.9	3.411	1.307	4.890	6.390	7.801	3.460
18	0.3	2000	40	4.8	4.8	39	3.090	1.288	4.041	5.204	6.324	3.740
19	0.4	1000	30	0.2	0.2	1.1	2.958	1.284	2.997	3.847	4.659	0.159
20	0.4	1000	35	1.3	1.3	12.4	3.171	1.270	5.117	6.499	7.760	0.989
21	0.4	1000	40	1.4	1.4	12.8	3.556	1.317	4.535	5.971	7.314	1.063
22	0.4	1500	30	2.9	2.9	21	2.813	1.262	3.588	4.528	5.424	2.266
23	0.4	1500	35	3	3	21.7	2.711	1.251	3.594	4.497	5.360	2.432
24	0.4	1500	40	3	3	25.2	3.005	1.275	4.419	5.634	6.794	2.318
25	0.4	2000	30	3.8	3.8	32.9	3.504	1.304	4.181	5.451	6.627	2.949
26	0.4	2000	35	3.8	3.8	30.9	3.489	1.305	3.976	5.190	6.317	2.881
27	0.4	2000	40	4.5	4.5	38.7	3.216	1.294	4.129	5.341	6.498	3.457

Figure. 7 and 8 depict the calculated values of statistical markers for EMD and LMD, respectively. to show the fluctuation in statistical characteristics with relation to the number of experiments The Nakagami probability distribution was utilised to set the statistical parameter thresholds in this strategy. The mean and standard deviation of the distributed data are here. The red line represents the statistical indicator's upper chatter threshold, while the green line represents the lower chatter threshold.

For example, in Fig. 7 (a) root mean square value vs experiment number plot for IMF, the top and lower threshold values are 3.87 and 0.66, respectively. The red line is drawn at 3.87 and the green line is drawn at 0.66 in the same plot. The experiment number that falls below the green threshold line resembles stable machining (machining without noise), whereas the experiment number that falls over the red threshold line resembles unstable machining (machining with clatter). The threshold of the other statistical indicator was calculated in the same way. In addition, stability charts for the list of experiments labelled stable, moderate, and unstable have been developed, as shown in Tables 4 and 5 for EMD and LMD, respectively. The trials that were recognised as stable by each statistical indicator were then classified as common experiments.

Table 1 Statistical indicators of prominent PFs

Exp. No.	(d) mm	(n) rpm	(f) mm/min	Standard deviation	RMS value	Peak-to-peak value	Kurtosis index	Waveform index	Peak index	Impulse index	Margin index	Absolute mean amplitude
1	0.2	1000	30	2.4	2.4	29.2	4.020	1.327	4.969	6.920	8.662	1.99
2	0.2	1000	35	2.3	2.3	29.6	4.001	1.321	5.655	6.791	8.699	1.76
3	0.2	1000	40	1.6	1.6	22.7	4.767	1.340	8.112	10.872	11.424	1.42
4	0.2	1500	30	3.6	3.6	47.9	4.260	1.315	6.902	9.147	11.176	2.73
5	0.2	1500	35	2.5	2.5	25.1	3.992	1.325	5.340	7.075	8.676	1.85
6	0.2	1500	40	2.5	2.5	24.5	3.741	1.317	4.673	6.153	7.528	1.87
7	0.2	2000	30	3.6	3.6	35.6	4.412	1.338	5.830	7.891	9.756	3.67
8	0.2	2000	35	4.1	4.1	40.9	3.987	1.333	4.849	6.462	7.968	3.07
9	0.2	2000	40	4.5	4.5	46.8	4.104	1.343	6.292	7.911	9.819	3.38
10	0.3	1000	30	1.5	1.5	22.7	5.226	1.350	8.304	11.208	11.830	1.10
11	0.3	1000	35	2.3	2.3	34.6	5.008	1.349	7.202	9.717	10.950	1.03
12	0.3	1000	40	1.6	1.6	18.2	3.961	1.324	6.004	7.952	9.762	1.22
13	0.3	1500	30	2.6	2.6	27.1	3.914	1.325	4.828	6.400	7.858	1.97
14	0.3	1500	35	1.8	1.8	15.5	3.273	1.282	4.677	5.994	7.208	1.40
15	0.3	1500	40	1.8	1.8	17.2	3.444	1.288	5.029	6.478	7.810	1.79
16	0.3	2000	30	4.7	4.7	41.8	3.896	1.336	4.431	5.919	7.326	3.48
17	0.3	2000	35	4.7	4.7	44.0	4.163	1.338	6.518	8.046	12.500	3.48
18	0.3	2000	40	4.9	4.9	43.2	3.719	1.330	4.271	5.682	7.026	3.72
19	0.4	1000	30	2.5	2.5	29.9	4.354	1.339	5.916	7.922	9.732	1.89
20	0.4	1000	35	2.4	2.4	32.5	4.539	1.338	7.601	8.041	9.853	1.77
21	0.4	1000	40	1.8	1.8	23.2	4.133	1.325	5.492	7.276	8.937	1.92
22	0.4	1500	30	3.1	3.1	38.8	3.720	1.311	5.739	7.522	9.214	2.34
23	0.4	1500	35	3.2	3.2	26.5	3.429	1.311	3.975	5.212	6.400	2.43
24	0.4	1500	40	3.1	3.1	30.5	3.580	1.319	4.900	6.466	7.969	2.34
25	0.4	2000	30	4.1	4.1	45.5	3.865	1.326	5.737	7.605	9.355	3.11
26	0.4	2000	35	4	4.0	39.5	3.856	1.325	4.958	6.567	8.072	3.02
27	0.4	2000	40	4.7	4.7	44.1	3.791	1.331	4.793	6.380	7.887	3.55

Furthermore, these common tests were compared to the theoretical stability lobe diagram in order to determine the statistical indicator of which preprocessed technique signal predicts stability more exactly. Figure 9 depicts the hypothesised stability lobe diagram. The green-colored tests in Fig. 9 are stable since they are below the curve. However, the red-colored experiments are unstable. Furthermore, the blue colour has been utilised to symbolise investigations on the edge of stability. When comparing the stability predicted using signals preprocessed using two distinct approaches, it was discovered that the LMD forecast is more accurate than the EMD prediction. Experiments 3, 4, 6, 20, 21, 24, 25, 26 should be stable/moderate stable, while experiments 1, 2, 5, 7, 8, 9, 10, 11, 12, 13, 14, 15, 16, 17, 18, 19, 22, 23, 27 should be unstable, according to the results obtained using the EMD technique, as shown in Table 6. When compared to the stability lobe diagram, it was discovered

that experiments 25 and 26 are in the unstable region. As a result, the prediction is ineffective. The mode mixing phenomena is one of the reasons behind this failure. Because the chatter signal has non-monotonous behaviour, the EMD approach occasionally fails to extract accurate characteristics. As indicated in Table 7, the stable/moderate stable experiments obtained in the case of LMD are 1, 2, 4, 5, 6, 8, 13, 19, 20, 22, 24, 26, and the

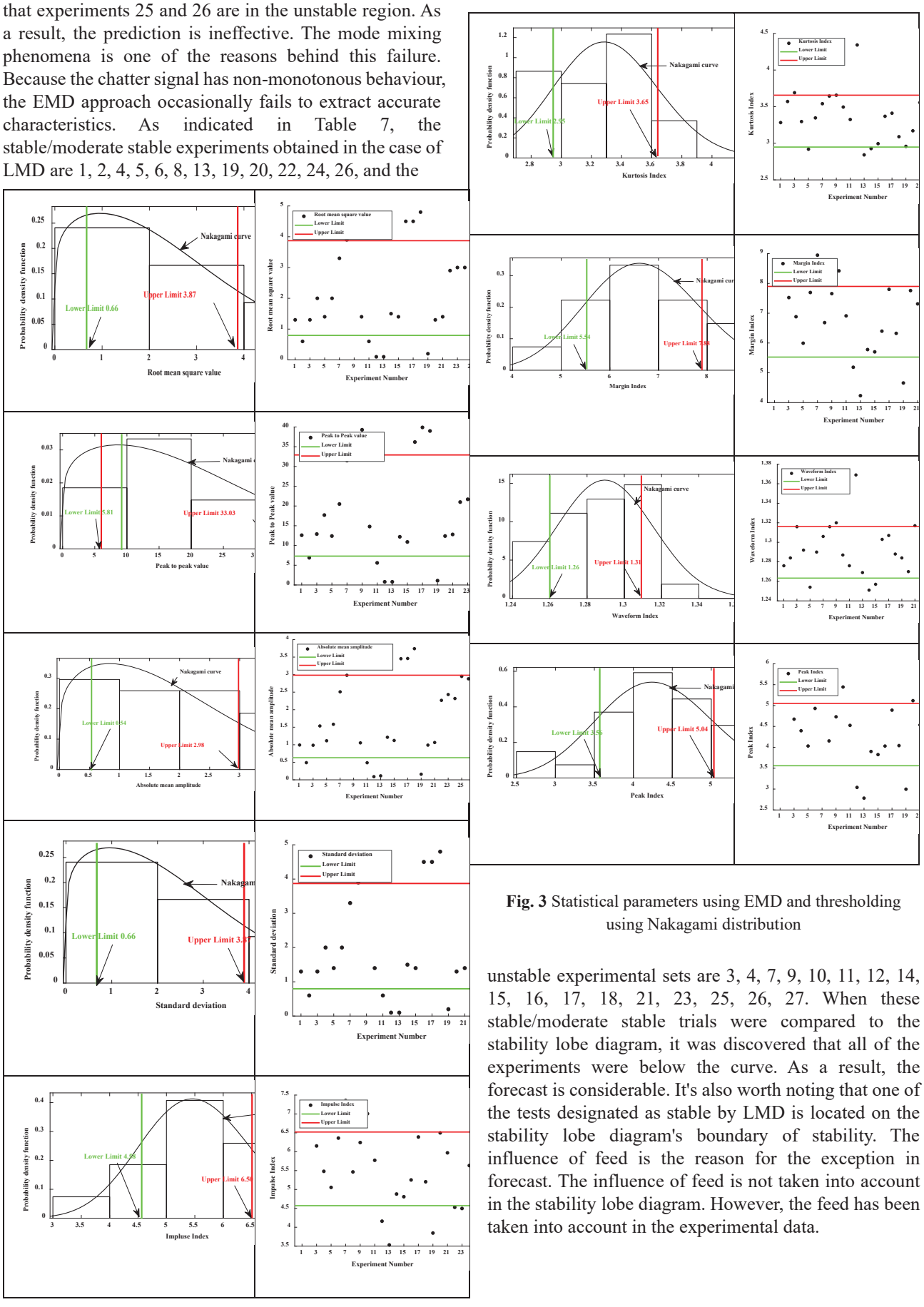

Fig. 3 Statistical parameters using EMD and thresholding using Nakagami distribution

unstable experimental sets are 3, 4, 7, 9, 10, 11, 12, 14, 15, 16, 17, 18, 21, 23, 25, 26, 27. When these stable/moderate stable trials were compared to the stability lobe diagram, it was discovered that all of the experiments were below the curve. As a result, the forecast is considerable. It's also worth noting that one of the tests designated as stable by LMD is located on the stability lobe diagram's boundary of stability. The influence of feed is the reason for the exception in forecast. The influence of feed is not taken into account in the stability lobe diagram. However, the feed has been taken into account in the experimental data.

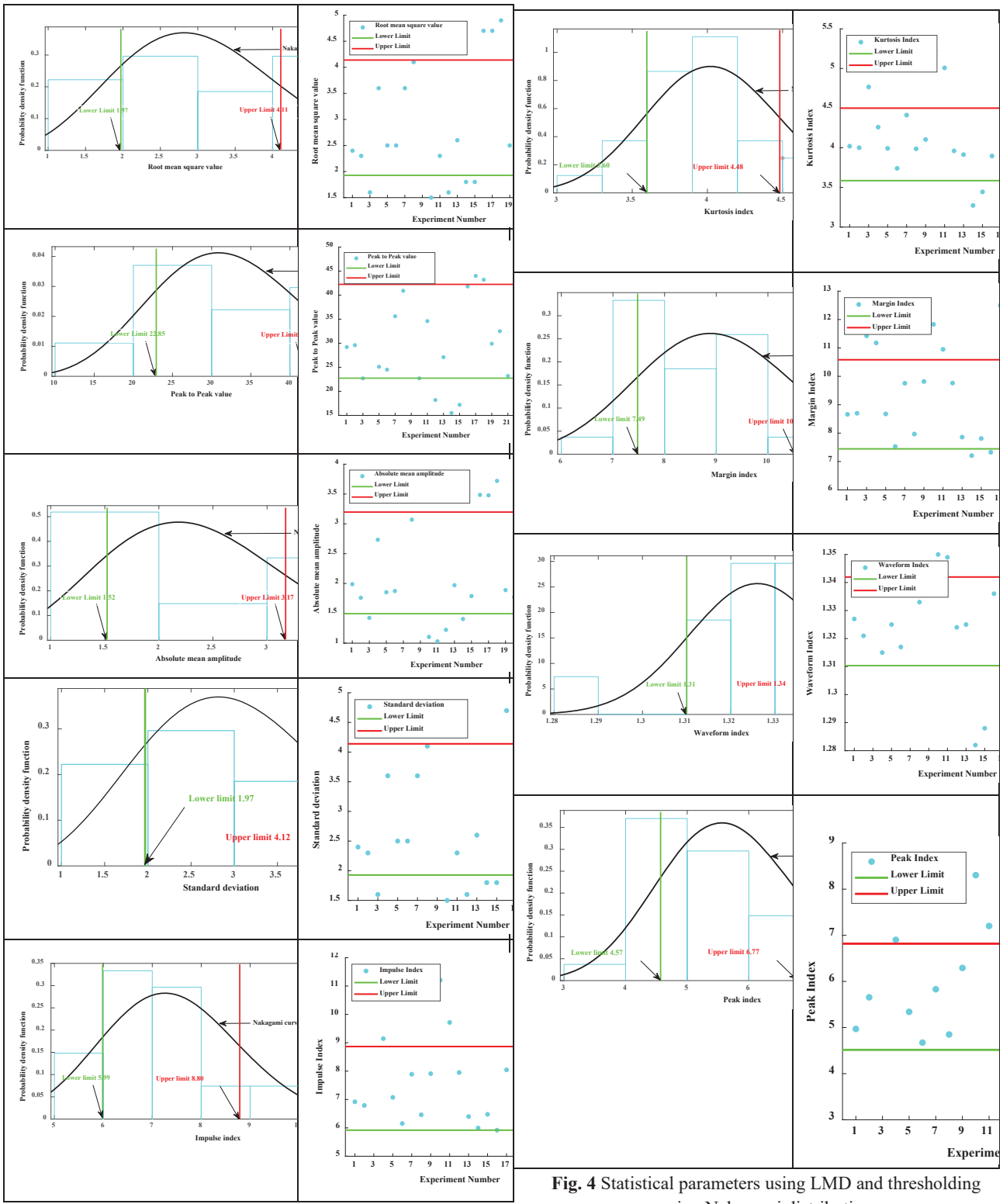

Fig. 4 Statistical parameters using LMD and thresholding using Nakagami distribution

Table 2. Prediction of stable and unstable experimental runs for EMD pre-processed signal

Statistical Indicator	Stable	Moderate	Unstable
RMS	1, 2, 4, 5, 6, 7, 11, 13, 19, 20, 22, 23, 24, 26	8, 25	3, 9, 10, 12, 14, 15, 16, 17, 18, 21, 27
Peak to Peak	1, 2, 5, 6, 7, 8, 11, 13, 19, 20, 22, 23, 24, 26	3, 4, 10, 16, 21	4, 9, 12, 14, 15, 17, 18, 25, 27
Absolute mean amplitude	1, 2, 4, 5, 6, 8, 13, 15, 19, 20, 21, 22, 23, 24, 26	25	3, 7, 9, 10, 11, 12, 14, 16, 17, 18, 27
Standard deviation	1, 2, 4, 5, 6, 7, 11, 13, 19, 20, 22, 23, 24, 26	8, 25	3, 9, 10, 12, 14, 15, 16, 17, 18, 21, 27
Impulse Index	1, 2, 5, 7, 8, 9, 12, 13, 15, 18, 19, 20, 21, 22, 24, 25, 26, 27	4, 6, 14, 16	3, 4, 10, 11, 17, 23
Kurtosis	1, 2, 4, 5, 6, 7, 8, 9, 12, 13, 16, 17, 18, 19, 21, 22, 25, 26, 27	20, 24	3, 10, 11, 14, 15, 23
Marginal Index	1, 2, 5, 7, 8, 9, 12, 13, 15, 19, 20, 21, 22, 24, 25, 26, 27	4, 6, 16	3, 4, 10, 11, 14, 17, 18, 23
Waveform Index	1, 2, 4, 5, 6, 7, 8, 12, 13, 16, 17, 18, 19, 20, 21, 24, 25, 26, 27	22, 23	3, 9, 10, 11, 14, 15
Peak Index	1, 2, 5, 7, 8, 9, 12, 13, 15, 17, 18, 19, 20, 21, 22, 24, 25, 26, 27	4, 6, 14, 16	3, 10, 11, 23
Common runs	1, 2, 5, 13, 19, 26	4, 6, 8, 20, 22, 24	3, 4, 7, 9, 10, 11, 12, 14, 15, 16, 17, 18, 21, 23, 25, 26, 27

Table 3. Prediction of stable and unstable experimental runs for LMD pre-processed signal

Statistical Indicator	Stable	Moderate	Unstable
RMS	1, 3, 4, 5, 6, 7, 10, 14, 15, 20, 21, 22, 23, 24	8, 25, 26	2, 9, 11, 12, 13, 16, 17, 18, 19, 27
Peak to Peak	1, 3, 4, 5, 6, 7, 8, 10, 14, 15, 20, 21, 22, 23, 24, 26	2, 25	9, 11, 12, 13, 16, 17, 18, 19, 27
Absolute mean amplitude	1, 3, 4, 5, 6, 7, 10, 14, 15, 20, 21, 22, 23, 24	8, 25, 26	2, 9, 11, 12, 12, 16, 17, 18, 19, 27
Standard deviation	1, 3, 4, 5, 6, 7, 10, 14, 15, 20, 21, 22, 23, 24	8, 25, 26	2, 9, 11, 12, 13, 16, 17, 18, 19, 27
Impulse Index	3, 4, 5, 6, 7, 8, 9, 10, 11, 14, 15, 16, 17, 18, 21, 24, 25, 26, 27	20, 22, 23	1, 2, 12, 13, 19
Kurtosis	1, 2, 4, 6, 7, 10, 11, 16, 17, 18, 20, 21, 25, 26, 27	3, 5, 8, 9, 14, 15, 19, 24	12, 13, 22, 23
Marginal Index	3, 4, 5, 6, 8, 9, 11, 14, 15, 16, 18, 21, 24, 25, 26, 27	17, 20, 22, 23	1, 2, 7, 10, 12, 13, 19
Waveform Index	1, 2, 4, 6, 7, 10, 11, 13, 16, 17, 18, 19, 20, 24, 25, 26, 27	3, 8, 9, 21, 22	5, 12, 14, 15, 23
Peak Index	3, 4, 5, 6, 7, 8, 11, 14, 15, 16, 17, 18, 21, 24, 25, 26, 27	20, 22, 23	1, 2, 9, 10, 12, 13, 19
Common runs	4, 6	3, 20, 21, 24, 25, 26	1, 2, 5, 7, 8, 9, 10, 11, 12, 13, 14, 15, 16, 17, 18, 19, 22, 23, 27

Table 4 Chatter prediction based on EMD

	No chatter	Moderate chatter	High chatter
Experimental runs	4, 6	3, 20, 21, 24, 25, 26	1, 2, 5, 7, 8, 9, 10, 11, 12, 13, 14, 15, 16, 17, 18, 19, 22, 23, 27

Table 5 Chatter prediction based on LMD

	No chatter	Moderate chatter	High chatter
Experimental runs	1, 2, 5, 13, 19, 26	6, 8, 20, 22, 24	3, 4, 7, 9, 10, 11, 12, 14, 15, 16, 17, 18, 21, 23, 25, 26, 27

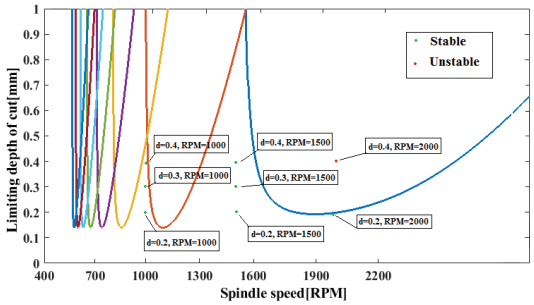

Fig. 5: Theoretical stability lobe diagram

3. Conclusions

The current study focuses on diagnosing tool chatter by acquiring audio chatter signals and pre-processing them using adaptive signal processing techniques. Furthermore, a comparison of the two adaptive approaches has been presented, with the following major findings:

1. The obtained raw chatter signals can be preprocessed using both EMD and LMD approaches. However, because to the phenomena of mode mixing, EMD sometimes fails to display the precise properties.
2. LMD has an advantage over EMD in that it can more precisely forecast the commencement of chatter by ignoring incipient amplitude changes in the signal.
3. Both approaches detect a buzz frequency of roughly 200 Hz. This indicates that chatter occurs at roughly 200 Hz for the specified set of cutting conditions.
4. The results also reveal that under the specified set of cutting settings and according to the defined experimental design. It is safe to undertake experiments 1, 2, 4, 5, 6, 8, 13, 19, 20, 22, 24, and 26.

The proposed methodology could serve as a guideline for researchers/machinists in terms of online monitoring and predicting which tests will not have chatter. The effect of feed can be considered in the near future for improved results.

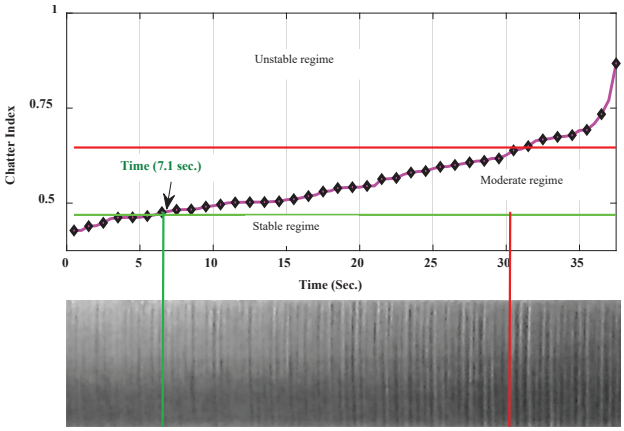

Fig. 6 Threshold of Chatter Index for online chatter detection

Funding: There has been no funding for this project from any organisation.

References

1) Filippov A, Nikonov AY, Rubtsov V, et al. Vibration and acoustic emission monitoring the stability of peakless tool turning: Experiment and modeling. 246: 224-234 (2017).
2) Gupta P and Singh B. Investigation of Tool Chatter Features at Higher Metal Removal Rate Using Sound Signals. Acoustics Australia: 1-8 (2020).
3) J. Munoa, X. Beudaert, Z. Dombovari, Y. Altintas, E. Budak, C. Brecher, G. Stepan, Chatter suppression techniques in metal cutting, CIRP Annals, (65) 785-808, (2016). doi:10.1016/2016.06.004
4) I. Mancisidor, A. Pena-Sevillano, Z. Dombovari, R. Barcena, J. Munoa, Delayed feedback control for chatter suppression in turning machines, Mechatronics, (63) 102276, (2019). doi:10.1016/2019.102276
5) N. Weake, M. Pant, A. Sheoran, A. Haleem, and H. Kumar, "Optimising parameters of fused filament fabrication process to achieve optimum tensile strength using artificial neural network," EVERGREEN Joint Journal of Novel Carbon Resource Sciences & Green Asia Strategy, 7 (3) 373–381 (2020). https://doi.org/10.5109/4068614
6) H. Han, M. Hatta, and H. Rahman, "Smart ventilation for energy conservation in buildings," EVERGREEN Joint Journal of Novel Carbon Resource Sciences & Green Asia Strategy, 6 (1) 44–51 (2019). doi:10.5109/2321005.
7) Gupta P and Singh B. Exploration of tool chatter in CNC turning using a new ensemble approach (2021).
8) Huang NE, Shen Z, Long SR, et al. The empirical mode decomposition and the Hilbert spectrum for nonlinear and non-stationary time series analysis. Proceedings of the Royal Society of London A: mathematical, physical and engineering sciences. The Royal Society, 903-995 (1998).

9) M. Wan, J. Feng, Y.-C. Ma, W.-H. Zhang, Identification of milling process damping using operational modal analysis, International Journal of Machine Tools and Manufacture, (122) 120-131, (2017).
10) Y. Yang, W.-H. Zhang, Y.-C. Ma, M. Wan, Chatter prediction for the peripheral milling of thin-walled workpieces with curved surfaces, International Journal of Machine Tools and Manufacture, (109) 36-48 (2016). doi:10.1016/2017.06.006
11) G. Quintana, J. Ciurana, Chatter in machining processes: A review, International Journal of Machine Tools and Manufacture, (51) 363-376, (2011). doi:10.1016/2011.01.001
12) T.N. Dief, and S. Yoshida, "System identification for quad-rotor parameters using neural network," EVERGREEN Joint Journal of Novel Carbon Resource Sciences & Green Asia Strategy,, 3 (1) 6–11 (2016). doi:10.5109/1657380.
13) M.A. Berawi, S.A.O. Siahaan, Gunawan, P. Miraj, and P. Leviakangas, "Determining the prioritized victim of earthquake disaster using fuzzy logic and decision tree approach," EVERGREEN Joint Journal of Novel Carbon Resource Sciences & Green Asia Strategy, 7 (2) 246–252 (2020). doi:10.5109/4055227.
14) Maamar A, Bouzgarrou BC, Gagnol V, et al. Time domain stability analysis for machining processes. Advances in Acoustics and Vibration. Springer, 77-88 (2017).
15) S. P. Dwivedi, N.K. Maurya, M. Maurya, Assessment of Hardness on AA 2014/Eggshell composite Produced Via Electromagnetic Stir Casting Method, EVERGREEN Joint Journal of Novel Carbon Resource Sciences & Green Asia Strategy, 6 (06), 285-294 (2019). https://doi.org/10.5109/2547354
16) M. Maurya, N. K. Maurya, V. Bajpai, Effect of SiC Reinforced Particle Parameters in the Development of Aluminium Based Metal Matrix Composite, EVERGREEN Joint Journal of Novel Carbon Resource Sciences & Green Asia Strategy, 6(3), 200-206 (2019). doi.org/10.5109/2349295
17) Quintana G and Ciurana J. Chatter in machining processes: A review. International Journal of Machine Tools and Manufacture (51) 363-376, (2011).
18) Sandoval S, Bredin M and De Leon PL. Using Linear Prediction to Mitigate End Effects in Empirical Mode Decomposition. 2018 IEEE Global Conference on Signal and Information Processing (GlobalSIP). IEEE, 281-285 (2018).
19) Shrivastava Y, Singh B and Sharma AJMTP. Identification of Chatter in Turning Operation using WD and EMD. (5), 23917-23926 (2018).
20) Siddhpura M, Siddhpura A and Paurobally R. Chatter stability prediction for a flexible tool-workpiece system in a turning process. The International Journal of Advanced Manufacturing Technology (92), 881-896 (2017).
21) Zaida H, Bouchelaghem AM and Chehaidia SE. Experimental Study of Tool Wear Evolution during Turning Operation Based on DWT and RMS. Defect and Diffusion Forum. Trans Tech Publ, 392-405 (2021).
22) H. Sosiati, Y. A. Shofie, A. W. Nugroho,Tensile Properties of Kenaf/E-glass Reinforced Hybrid Polypropylene (PP) Composites with Different Fiber Loading, EVERGREEN Joint Journal of Novel Carbon Resource Sciences & Green Asia Strategy, 05, (2) 1-5 (2018). https://doi.org/10.5109/1936210
23) A. K. Srivastava, S. P. Dwivedi, N. K. Maurya, Manish Maurya, 3D visualization and topographical analysis in turning of hybrid MMC by CNC lathe SPRINT 16TC made of BATLIBOI, EVERGREEN Joint Journal of Novel Carbon Resource Sciences & Green Asia Strategy, 07, (02), 202-208, (2020) https://doi.org/10.5109/4055217
24) R. Rafal, L. Pawel, K. Krzysztof, K. Bogdan, W. Jerzy, Chatter identification methods on the basis of time series measured during titanium superalloy milling, International Journal of Mechanical Sciences, (99),196-207 (2015). doi:10.1016/2015.05.013
25) C. Liu, L. Zhu, C. Ni, The chatter identification in end milling based on combining EMD and WPD, The International Journal of Advanced Manufacturing Technology, (91), 3339-3348 (2017). doi:10.1007/00170-017-0024-8
26) Zhang Z, Li H, Meng G, et al. Chatter detection in milling process based on the energy entropy of VMD and WPD. International Journal of Machine Tools and Manufacture (108), 106-112 (2016).